Control of the Area Density of Vertically Grown ZnO Nanowires by Blending PS-*b*-P4VP and PS-*b*-PAA Copolymer Micelles

Wonseok Hwang,[†] Ji-Hyuk Choi,[†] Tae Hee Kim,[†] Jinwoo Sung,[†] Jae-Min Myoung,[†] Dae-Geun Choi,[‡] Byeong-Hyeok Sohn,[§] Sang Soo Lee,[||] Dong Ha Kim,[⊥] and Cheolmin Park*[,†]

Department of Materials Science and Engineering, Yonsei University, Seoul, 120-749, Korea, Nano-Mechanical Systems Research Center, Korea Institute of Machinery & Materials, 171 Jang-dong, Yuseong-gu, Daejeon, 305-343 Korea, Department of Chemistry, Seoul National University, Seoul, Korea, Polymer Hybrid Research Center, Korea Institute of Science and Technology, P.O. Box 131, Cheongryang, Seoul 130-650, Korea, and Division of Nano Sciences and Department of Chemistry and Nano Science Ewha Womans University, 11-1 Daehyun-Dong, Seodaemun-Gu, Seoul 120-750, Korea

Received March 11, 2008. Revised Manuscript Received May 14, 2008

We develop a novel and simple method for controlling the area density of ZnO nanowires vertically grown on a Si substrate. The method is based on blending spherical polystyrene-*block*-poly(acrylic acid) (PS-*b*-PAA) micelles with polystyrene-*block*-poly 4-vinylpyridine (PS-*b*-P4VP) for the area density control of Au nanoparticles, a catalyst of ZnO nanowires, chemically reduced from hydrogen tetrachloroaurate ($HAuCl_4$) selectively in P4VP core block. No interdiffusion between the two types of block copolymer micelles allows us to fabricate the monolayer of the mixed micelles with the controlled density of Au nanoparticles from which single crystal ZnO nanowires are grown by the VLS method. The number of ZnO nanowires per unit area varies from approximately $15-120\ \mu m^{-2}$ with a tuning capability of more than 800%. Micropatterns with the controlled density of Au nanoparticles are also fabricated by selective pattern transfer of blended micelles.

Introduction

Nanowires vertically grown on a substrate have been of great interest for potential applications of electron emitters for display, highly sensitive detectors for biosensors, carrier channels for vertical transistors, and so on.[1–3] In particular, nanowires grown in general from metallic nanoparticle catalysts such as Au, Ni, and Fe provide further benefits because they can be deposited on versatile substrates. There are two main methods for the formation of nanoparticle catalysts on a substrate: dewetting of a thin metallic film and spreading of nanoparticles ex situ synthesized.[4,5] In the first method, hemispherical nanoparticle domains are developed and self-organized during thermally induced dewetting of a thin metal layer and their size and distribution on a substrate is fairly uniform. The nanoparticles are closely packed with each other, leading to a peudo hexagonal packing. In the other way, a solution of catalytic nanoparticles synthesized and dispersed in an organic solvent is spin cast, giving rise to a monolayer of closed packed particles after solvent evaporation.

Another way to fabricate vertically grown nanowires from catalytic nanoparticles is the use of polymeric micelles selectively containing metallic nanoparticles in their core regions.[6,7] Amphiphilic block copolymers are easily self-assembled into micelles in nonpolar medium where polar blocks aggregated inside form the core of a micelle with the corona consisting of nonpolar ones. Well-known coordination of metallic salts such as hydrogen tetrachloroaurate(III) trihydrate ($HAuCl_4 \cdot 3H_2O$), silver acetate (AgAc), silver nitrate ($AgNO_3$), and so on into polar blocks allows the formation of various nanoparticles in the core. Nanoparticles encapsulated into block copolymer micelles have been utilized for fabricating nanowire arrays vertically grown on several substrates.[8–12]

Controlled growth of nanowires has gained a great attention in which both position and density of nanowires are regulated in certain manners. The micropatterned nanowires and nanotubes have been usually achieved by micro-

* Corresponding author. Tel: 82-2-2123-2833. Fax: 82-2-312-5375. E-mail: cmpark@yonsei.ac.kr.
[†] Yonsei University.
[‡] Korea Institute of Machinery & Materials.
[§] Seoul National University.
[||] Korea Institute of Science and Technology.
[⊥] Ewha Womans University.

(1) Duan, X.; Huang, Y.; Cui, Y.; Wang, J.; Lieber, C. M. *Nature* **2001**, *409*, 66.
(2) Wang, W. U.; Chen, C.; Lin, K.; Fang, Y.; Lieber, C. M. *Proc. Natl. Acad. Sci. U.S.A.* **2005**, *102*, 3208.
(3) Goldberger, J.; Hochbaum, A. I. ; Fan, R.; Yang, P. *Nano Lett.* **2006**, *6*, 973.
(4) Yang, P. D.; Yan, H. Q.; Mao, S.; Russo, R.; Johnson, J.; Saykally, R.; Morris, N.; Pham, J.; He, R. R.; Choi, H. J. *Adv. Funct. Mater.* **2002**, *12*, 323.
(5) Cui, Y.; Lauhon, L. J.; Gudiksen, M. S.; Wang, J.; Lieber, C. M. *Appl. Phys. Lett.* **2001**, *78*, 2214.
(6) Lu, J. Q.; Yi, S. S. *Langmuir* **2006**, *22*, 3951.
(7) Fu, Q.; Huang, S.; Liu, J. *J. Phys. Chem. B* **2004**, *108*, 6124.
(8) Hwang, W.; Ham, M. H.; Sohn, B. H.; Huh, J.; Kang, Y. S.; Jeong, W.; Myoung, J. M.; Park, C. *Nanotechnology* **2005**, *16*, 2897.
(9) Bennett, R. D.; Xiong, G. Y.; Ren, Z. F.; Cohen, R. E. *Chem. Mater.* **2004**, *16*, 5589.
(10) Glass, R.; Möller, M.; Spatz, J. P. *Nanotechnology* **2003**, *14*, 1153.
(11) Gorzolnik, B.; Mela, P.; Möller, M. *Nanotechnology* **2006**, *17*, 5027.
(12) Glass, R.; Arnold, M.; Blümmel, J.; Küller, A.; Möller, M.; Spatz, J. P. *Adv. Funct. Mater.* **2003**, *13*, 569.

10.1021/cm800719h CCC: $40.75
Published on Web 09/19/2008

patterning catalytic nanoparticles using microcontact printing, photolithography, solvent capillary contact printing, and e-beam lithography followed by nanowire growth.[8,12–14] Although these micropatternings of the catalytic nanoparticles offer convenient ways for patterned nanowire arrays, the consequent nanowires in the micropatterned regions are hardly controlled in area density of the nanowires because of their closed-packed and templated structure arising from the self-assembled nanostructure of the catalytic particles beneath.

Controlling the domain-domain period (i.e., center-to-center distance of two nanoparticles, *d*) of nanowires has been achieved by a few methods. Simply, changing concentration of solution of catalytic nanoparticles can manipulate *d*. The method is, however, practically limited to length scales a little larger than the period determined by closed packing of the nanoparticles because it is difficult to evenly spread the nanoparticles on a substrate in particular at low concentration of solution with the narrow distribution of the average value of *d*. The spin coating of the solution with low concentration frequently results in aggregates of the nanoparticles. The area density control of nanowires and tubes was also accomplished by varying the seed layer thickness.[15] Wang et al. have demonstrated that the dewetting kinetics of catalytic Au layer depends on the layer thickness and thus the resulting variation of the size and distribution of Au nanoparticles allows the size- and area-controlled ZnO nanowire growth.[15]

Another strategy for the area density control of nanowires is based on block copolymer micelles. The method is to control the corona thickness of a nanoparticle containing block copolymer micelle, which scales with the molecular weight of the outer block and thus to regulate the average distance of nanowires. The way is simpler but the allowed tuning range is limited roughly to 100−150% of the inherent size of *d* because of the difficulty in synthesizing a block copolymer with extremely high molecular weight ($\sim 1 \times 10^6$ g/mol). The block copolymer micelles containing catalytic nanoparticles for nanowires were also mixed with homopolymer compatible with the corona of the micelles for controlling the density of the catalytic nanoparticles.[16] The area density of catalytic Fe ions for carbon nanotube synthesis selectively located in the block copolymer micelles was also controlled with blending homopolymer compatible with the corona block of the micelle.[16] The method, however, seems to be difficult to obtain reasonably uniform micelle-to-micelle distance in particular when the portion of a homopolymer in the blend is high. In addition, a possible macrophase separation between the homopolymer and the block copolymer may occur.

Blending two types of block copolymer micelles in solution or air/water interface has been considered as an effective way for fabricating new nano-objects that cannot be obtained with single micelle systems and for manipulating fluorescence of dyes with different emission maximum confined respectively into the cores of the micelles.[17] In this contribution, we utilize the blending of two types of block copolymer micelles, one of which contains catalytic Au nanoparticles in its core, to control the density of nanowires vertically grown on a substrate. Spin casting of a micelle mixture with various blend ratios allows us to systematically tune the area density of the nanoparticles from which ZnO nanowires are subsequently grown with the controlled density.

Experimental Section

Materials and Micelle Blending. We employed two amphiphilic block copolymers: Poly(styrene-*block*- 4-vinyl pyridine) (PS-*b*-P4VP, 47 600−20 900 g/mol) and Poly(styrene-*block*- acrylic acid) (PS-*b*-PAA, 16 500−4300 g/mol) purchased from Polymer Source Inc., Dorval, Canada. Polydispersity Indices (PDI) of two block copolymers were 1.14 and 1.15, respectively. Two block copolymers were dissolved in toluene with 0.5 wt % at 80 °C for 30 min. This condition was well-developed to obtain a micelle solution in which nonpolar (PS) corona and polar (P4VP and PAA) core micelle were readily formed. Two different micelle solutions were blended with different volume compositions (PS-*b*-P4VP/PS-*b*-PAA) from 1/9 to 9/1.

ZnO Synthesis. Hydrogen tetrachloroaurate(III) trihydrate ($HAuCl_4 \cdot 3H_2O$), a precursor for Au catalyst for ZnO nanowires was purchased from Sigma-Aldrich (99.99%) and ZnO powders were obtained from Sigma-Aldrich Co. of $HAuCl_4 \cdot 3H_2O$ (0.5 equiv.) with respect to P4VP block was dissolved with PS-*b*-P4VP micelles in toluene. The $HAuCl_4 \cdot 3H_2O$ selectively loaded in P4VP cores was subsequently reduced to Au nanoparticles. A mixture of PS-*b*-P4VP micelles with Au nanoparticles and PS-*b*-PAA ones was spin coated on Si substrates with 2000 rpm for 60 s and a thin monolayered micelle film was subsequently formed. The ZnO nanowires were synthesized from the Au nanoparticles in P4VP cores as catalysts by VLS method of ZnO powder in a horizontal tube furnace under Ar gas flow with a rate of 30 sccm at 1000 °C for 30 min. Blended block copolymer micelle thin films on Si (100) substrate were located at the downstream of the furnace with a separation of about 100 mm away from the sources, i.e., at the colder zone near the venting outlet. After the synthesis process, white products were obtained on the substrates. All blended micelle thin films were located at the same position and growth temperature and time were also identically controlled. Figure 1 is a schematic diagram of ZnO nanowires vertically grown with controlled area density by blending two types of block copolymer micelles.

Characterization. The size of two block copolymer micelles were characterized by dynamic light scattering (Malvern CGS-3) with $\lambda = 633.2$ nm and a scattering angle of 90°. Intensity autocorrelation functions $g^{(2)}(t)$ were recorded at room temperature. Correlation function $g^{(1)}(t)^2$ was related by $g^{(2)}(t) - 1 = g^{(1)}(t)^2$ with the minimum deviation from the ideal correlation and was plotted as a function of time. Inverse Laplace transformations were performed using the constrained regularization calculation program REPES to obtain the distribution of relaxation times, $G(\Gamma)$, where Γ is relaxation time. In addition, the diameter of micelles was analyzed with an atomic force microscope (AFM) in tapping mode (Nanoscope IVa, Digital Instrument) and a high-resolution field effect transmission electron microscope (FETEM) (Jeol 2100F). TEM samples were prepared by carbon coating the thin block

(13) Hochbaum, A. I.; Fan, R.; He, R.; Yang, P. *Nano Lett.* **2005**, *5*, 457.
(14) Lu, J.; Yi, S. S.; Kopley, T.; Qian, C.; Liu, J.; Gulari, E. *J. Phys. Chem. B* **2006**, *110*, 6655.
(15) Wang, X.; Song, J,.; Summers, C. J.; Ryou, J. H.; Li, P.; Dupuis, R. D.; Wang, Z. L. *J. Phys. Chem. B* **2006**, *110*, 7720.
(16) Bennett, R. D.; Hart, A. J.; Cohen, R. E. *Adv. Mater.* **2006**, *18*, 2274.
(17) Yoo, S. I.; An, S. J.; Choi, G. H.; Kim, K. S.; Yi, G. C.; Zin, W. C.; Jung, J. C.; Sohn, B. H. *Adv. Mater.* **2007**, *19*, 1594.

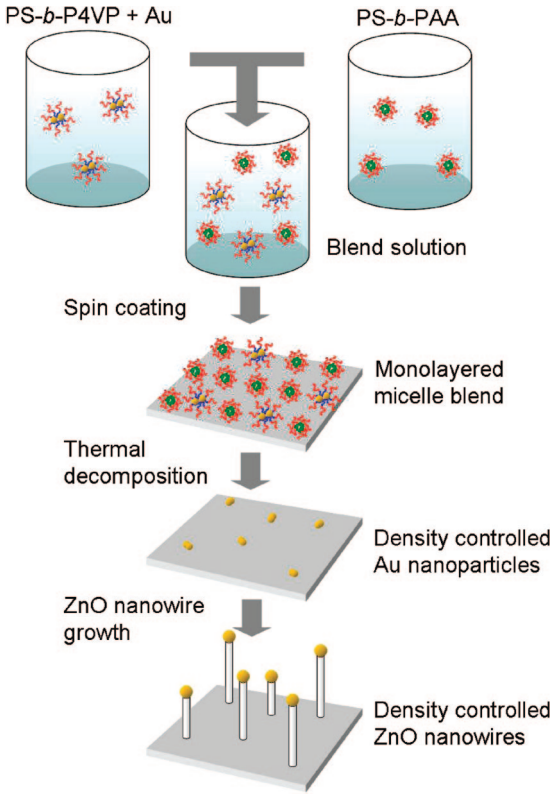

Figure 1. Schematic of the fabrication of ZnO nanowires with the area density controlled by blending two types of block copolymer micelles: PS-*b*-P4VP and PS-*b*-PAA. A mixture is formed of PS-*b*-PAA micelles and PS-*b*-P4VP containing Au nanoparticles in the P4VP cores reduced from metal salts. Spin coating of the mixture produces thin monolayered micelle films in which the area density of Au nanoparticles is controlled as a function of the blend ratios. The subsequent growth of nanowires using the catalytic Au nanoparticles gives rise to ZnO nanowires vertically grown with the controlled area density of the nanowires.

copolymer micelle film formed on either a mica sheet or Si substrate. Subsequently small sections of the carbon and polymer films were detached from the substrate employing poly(acrylic acid) (PAA) solution. After dissolution of the PAA, film sections were picked up by TEM grids.[8] ZnO nanowires on substrates were characterized with a scanning electron microscope (SEM) (Hitachi H-4200) and their crystal structure was analyzed with X-ray diffractometer (Kogaku Co. Ltd.) and FETEM.

Microtransfer Printing. Micropatterning of the blended block copolymer micelle films was performed by microtransfer printing developed in our laboratory. Polydimethlysiloxane (PDMS) prepolymer and curing agent kit (Sylgard 184, Dow Corning) were mixed with weight 10 to 1 and poured on the submicrometer master pattern; they were then cured at 80 °C for 6 h. The blended micelle solution was diluted to 0.2 wt % and dropped on the patterned PDMS mold and spin coated at 3000 rpm for 60 s. Thin film selectively formed on the protruding regions of the PDMS mold was transferred on Si wafer by conformal contact and subsequent transfer step after 3 min. The micropatterns formed were characterized by Optical microscope (OM: Olympus BX 51), AFM, and TEM.

Results and Discussion

The control of the interparticle distance of the catalytic Au nanoparticles by blending block copolymer micelles requires two conditions. First, a bimodal distribution should be obtained between the two types of micelles because hybrid micelles by molecular mixing of the two block copolymers gives rise to Au nanoparticles located in every micelle. Second, even in a bimodal distribution, metallic salt, a precursor of Au nanoparticles, should not be interdiffused between the two micelles. In general, the comicellization frequently occurs with a mixture of two micelles with the same constituent blocks, leading to hybrid micelles.[18] The hybrid micelles were also formed between two block copolymers with different corona block.[19,20] The bimodal distribution of two distinct block copolymer micelles has been achieved by various mixing protocols such as mixing from a micellar and a powdery state. In our recent work, we also systematically investigated the mixtures of two types of micelles with the identical molecular structure but different molecular weight and found that the formation of micelle solution with bimodal distribution strongly depended on the mixing protocols applied.[21]

The issue of the interdiffusion of metallic salts or Au nanoparticles became more serious even in a bimodal micelle solution with two PS-*b*-P4VP block copolymers having different molecular weight. For instance, when the micelles of PS-*b*-P4VP containing Au nanoparticles were mixed with those of another PS-*b*-P4VP having different molecular weight and composition (20 000−19 000 g/mol), the interdiffusion of the Au nanoparticles always took place, leading to homogeneous distribution of the nanoparticles in both micelles regardless of the mixing ratio of the two solutions. To avoid the possible comicellization and interdiffusion of Au nanoparticles, we utilized two different block copolymer micelles: PS-*b*-P4VP and PS-*b*-PAA in toluene with the same corona block of PS. The same corona block in the two micelles provides a homogeneous micelle-micelle interface with rare comicellization. In addition, no capability of loading $HAuCl_4$ salts into PAA core regions allows us to prevent Au nanoparticles selectively presynthesized in the P4VP core regions from the interdiffusion into the PAA cores.

First of all, we characterized the solution behavior of a mixture of the two micelles by dynamic light scattering (DLS). Figure 2 shows the DLS results obtained from PS-*b*-P4VP, PS-*b*-PAA, and a PS-*b*-P4VP/PS-*b*-PAA (7/3) blend solution aged for a week at a scattering angle of 90°. Figure 2a exhibits the correlation functions as a function of time that is related to the average micelle size. The decaying behavior of correlation function of the blend solution lies between that of a pure PS-*b*-PAA and that of a pure PS-*b*-P4VP and remains unchanged for a week, which indicates that the mixture of the two block copolymer micelles seems to stay independently in the solution rather than to interdiffuse with each other. Inverse Laplace transformations performed using the constrained regularization calculation offered the distribution of relaxation times which reflects the size distribution of the micelles.[22] The plot of PS-*b*-P4VP

(18) Honda, C.; Yamamoto, K.; Nose, T. *Polymer* **1996**, *37*, 1975.
(19) Stepanek, M.; Podhajecka, K.; Tesarova, E.; Prochazka, K.; Tuzar, Z.; Brown, W. *Langmuir* **2001**, *17*, 4240.
(20) Konak, C.; Helmstedt, M. *Macromolecules* **2003**, *36*, 4603.
(21) Yoo, S. I.; Sohn, B. H.; Zin, W. C.; Jung, J. C.; Park, C. *Macromolecules* **2007**, *40*, 8323.
(22) Li, Z.; Hillmyer, M. A.; Lodge, T. P. *Macromolecules* **2006**, *39*, 765.

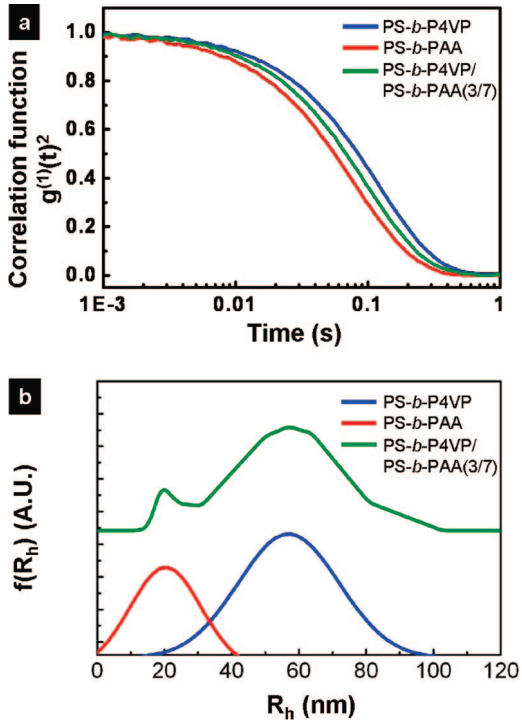

Figure 2. Dynamic light scattering results for PS-*b*-P4VP, PS-*b*-PAA, and a blended PS-*b*-P4VP/PS-*b*-PAA (3/7) micelle mixture: (a) correlation functions, $g^{(1)}(t)^2$ as a function of time and (b) distributions of the size of two types of block copolymer micelles. The curves are arbitrarily shifted for clarity. The scattering angle is fixed at 90°.

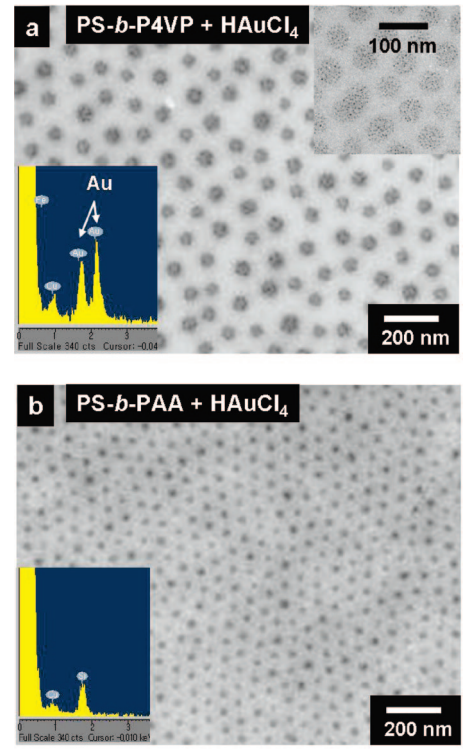

Figure 3. Bright-field TEM micrographs of (a) PS-*b*-P4VP and (b) PS-*b*-PAA micelles. The interdistance of the PS-*b*-PAA and PS-*b*-P4VP micelles was about 50 and 100 nm, respectively. Au nanoparticles were reduced only in the P4VP core and were not detected in PAA cores of PS-*b*-PAA micelles. Raspberry type Au nanoparticles in individual micelles are apparent in the right upper inset of Figure 3a. EDX spectra for each block copolymer micelle are shown in the left lower insets of (a) and (b).

and PS-*b*-PAA micelles in Figure 2b shows the distribution of the individual block copolymer micelles from which the averaged radii of PS-*b*-P4VP and PS-*b*-PAA micelles are obtained to be approximately 57 and 21 nm, respectively. It is noteworthy that a small amount of PS-*b*-PAA micelle scattering population in a solution mixture with 70% PS-PAA is due to mass-weighting of the scattering signal as previously demonstrated.[23] In addition, the presence of some cylindrical PS-*b*-PAA micelles as will be shown later is obviously influential on scattering signal in particular at high concentration regime, which usually leads to a possible overestimation of the radius of PS-*b*-PAA.

The size distribution plot of the PS-*b*-P4VP/PS-*b*-PAA (7/3) blend solution aged for 7 days clearly shows the bimodal distribution of the micelles with the characteristic radii of PS-*b*-P4VP and PS-*b*-PAA micelles, which confirms the negligible interdiffusion between the two micelles. Two facts are well-known: first of all, the kinetics of comicellization is in general rather slow (orders of hours and days), and chain interchange and mixing does not take place when core blocks are kinetically frozen due to highly nonsolvating medium.[19] In our system, both P4VP and PAA core blocks are almost kinetically frozen in a nonpolar toluene environment. We, therefore, draw the conclusion that two types of micelles stay independently in a blend solution, which allows us to fabricate monolayered blend films by spin coating as shown later.

The diameter of micelles depends mainly on the aggregation numbers influenced by the chemical structure of a block copolymer. In general, the aggregation number for an amphiphilic block copolymer is calculated by $Z = Z_0(N_A^{\alpha}N_B^{-\beta})$, where N_A and N_B are the degree of polymerization of insoluble and soluble block.[20,21] For the micellar systems, the exponents of α and β are close to 2.0 and 0.8, respectively. In particular, the experimental values for PS-*b*-P4VP/toluene solution were reported to be $\alpha = 1.93$ and $\beta = 0.79$. The parameter Z_0 is related to thermodynamic quantities such as an interaction parameter and a local packing parameter, and was reported as 1.66 for the PS-*b*-P4VP/toluene system.[21] In addition, Halperin theory represents the scaling relationship for the core radius of a starlike micelle expressed by $R \approx N_A^{4/25}N_B^{3/5}a$, where a is typical monomer size.[24] The core radii of PS-*b*-P4VP and PS-*b*-PAA micelles we observed are well-matched with the theoretical values.

The bright-field TEM images in images a and b in Figure 3 show monolayered PS-*b*-P4VP and PS-*b*-PAA micelles spin coated on Si substrates, respectively. The hydrodynamic radius of PS-*b*-P4VP micelles measured by DLS was approximately 57 nm in solution. Because the swollen PS coronas in toluene were collapsed and vitrified during spin coating by rapid solvent evaporation, the diameter of the P4VP cores and the center-to-center distance of two micelles become approximately 50 and 100 nm in the monolayer, respectively (Figure 3a). From the similar reason for PS-*b*-PAA micelles, the diameter of PS-*b*-PAA micelle core and the center-to-center distance was approximately 20 and 50

(23) Liu, T.; Nace, V. M.; Chu, B. *Langmuir* **1999**, *15*, 3109.

(24) Halperin, A. *Macromolecules* **1987**, *20*, 2943.

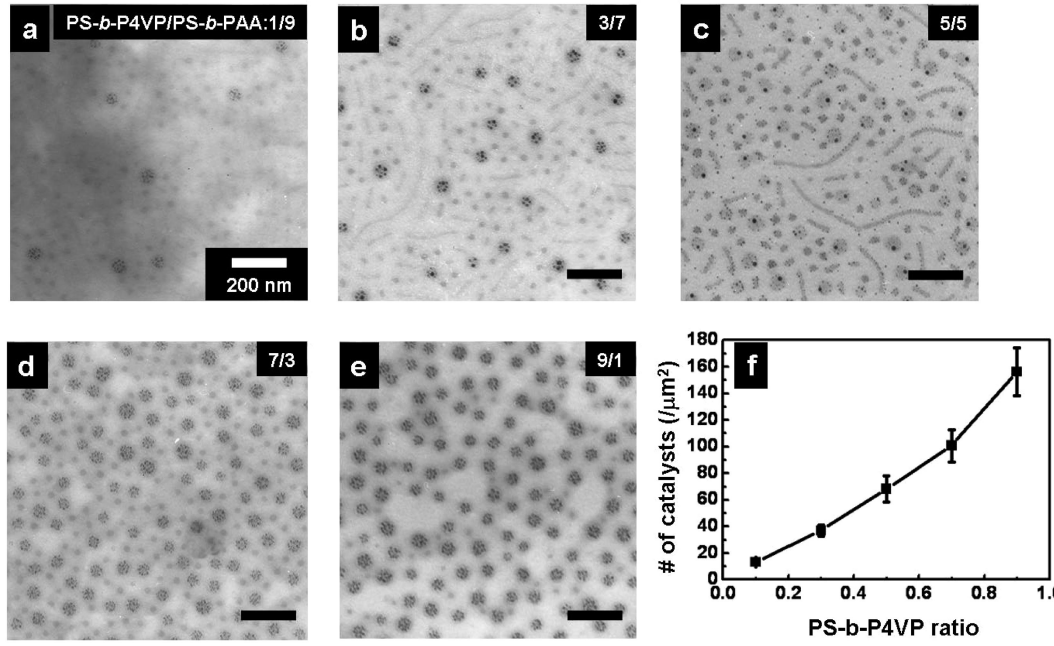

Figure 4. (a−e) Bright-field TEM micrographs of the PS-*b*-P4VP/PS-*b*-PAA blend films with different blend ratios. The number of Au nanoparticles in the P4VP cores increases with the change of blend ratio. Each core size was about 20 and 50 nm in diameter, respectively. (f) A plot of area density of Au nanoparticles in the P4VP cores of PS-*b*-P4VP micelles as a function of the blend ratios.

nm, respectively as shown in Figure 3b. For the center-to-center distance between micelles, both the length of corona chain proportional to N_B and the volume of core regions, $4\pi R_c^3/3 = ZN_AU_A$, are crucial, where R_c and U_A are the radius of the micelle core and the molar volume of core monomers, respectively.[25] Because the aggregation number and the radius of cores increase with the degree of polymerization of core blocks, we can easily expect that the core size of PS-*b*-P4VP micelles is larger than that of PS-*b*-PAA.

We selectively loaded Au nanoparticles in the P4VP cores of PS-*b*-P4VP micelles by the reduction of the $HAuCl_4$ $3H_2O$ metal salt as shown in Figure 3a. Au nanoparticles synthesized in the PS-*b*-P4VP micelles have a raspberry structure as visualized with dark spots in micelle cores in the inset of Figure 3a. The selective coordination of $HAuCl_4 \cdot 3H_2O$ in the P4VP blocks is attributed to the lone pair electrons in pyridine units of P4VP blocks easily protonated with $AuCl_4^-$ ions. On the contrary, the hydrophilic PAA blocks in the PS-*b*-PAA did not produce Au nanoparticles because of the lack of capability for protonatiing $AuCl_4^-$ ions. Polymers including P4VP and PEO are capable of interacting with acid metallic salts such as $HAuCl_4 \cdot 3H_2O$ and form anionic metallic complexes which are subsequently reduced into various nanoparticles with ease. Other metal salts that cannot make anionic metallic complex such as AgAc will not be coordinated in P4VP cores but can be in PAA cores instead. It is noted that the contrast in Figure 3b arises from the mass contrast of electron beam, which depends on the mass density of a sample. Energy-dispersive X-ray spectroscopy (EDX) analysis confirmed Au nanoparticles loading selectively in the P4VP cores of monolayered PS-*b*-P4VP micelle film. The characteristic X-ray peaks of Au are observed at 2.19 eV as shown in the inset of Figure 3a. Moreover, no characteristic peak of chlorine in $AuCl_4^-$ is detected because of the complete reduction of Au ions.[26,27] As expected, EDX data shown in the inset of Figure 3b for PS-*b*-PAA micelles did not show any characteristic emissions for Au nanoparticles.

Spin coating of a blend of Au nanoparticle loaded PS-*b*-P4VP and PS-*b*-PAA micelles allows us to control the area density of Au nanoparticles on a substrate. Figure 4a−e shows that the amount of Au nanoparticles selectively located in PS-*b*-P4VP micelles increases with the portion of PS-*b*-P4VP in the blends. A PS-*b*-P4VP/PS-*b*-PAA (1/9) blend in Figure 4a exhibits an average number density of the nanoparticles of approximately 15 μm^{-2}. The area density calculated by counting the number of micelles containing Au nanoparticles per unit area from several TEM micrographs increases with the blend ratio of PS-*b*-P4VP to PS-*b*-PAA and becomes 150 μm^{-2} in the ratio of 0.9, as shown in Figure 4f. The plot shown in Figure 4f indicates the area density of the nanoparticles almost linearly changed with the blend ratio. The relatively narrow standard deviations of nanoparticle-to-particle distance calculated in the micelle blends show no indication of a possible macrophase separation of the two micelles. The bimodal distribution of the two micelles in solution was preserved without intermicelle diffusion driven possibly by the capability of hydrogen bonding between basic moiety of P4VP and acidic moiety of PAA during spin coating. The difference of the two micelles in size led to the blend micelle structure with the less-perfect hexagonal packing. It should be also noted that the short cylindrical micelles of PS-*b*-PAA in images b and

(25) Förster, S.; Zisenis, M.; Wenz, E.; Antonietti, M. *J. Chem. Phys.* **1996**, *104*, 9956.
(26) Aizawa, M.; Buriak, J. M. *J. Am. Chem. Soc.* **2006**, *128*, 5877.
(27) Chai, J.; Wang, D.; Fan, X.; Buriak, J. M. *Nat. Nanotechnol.* **2007**, *2*, 500.

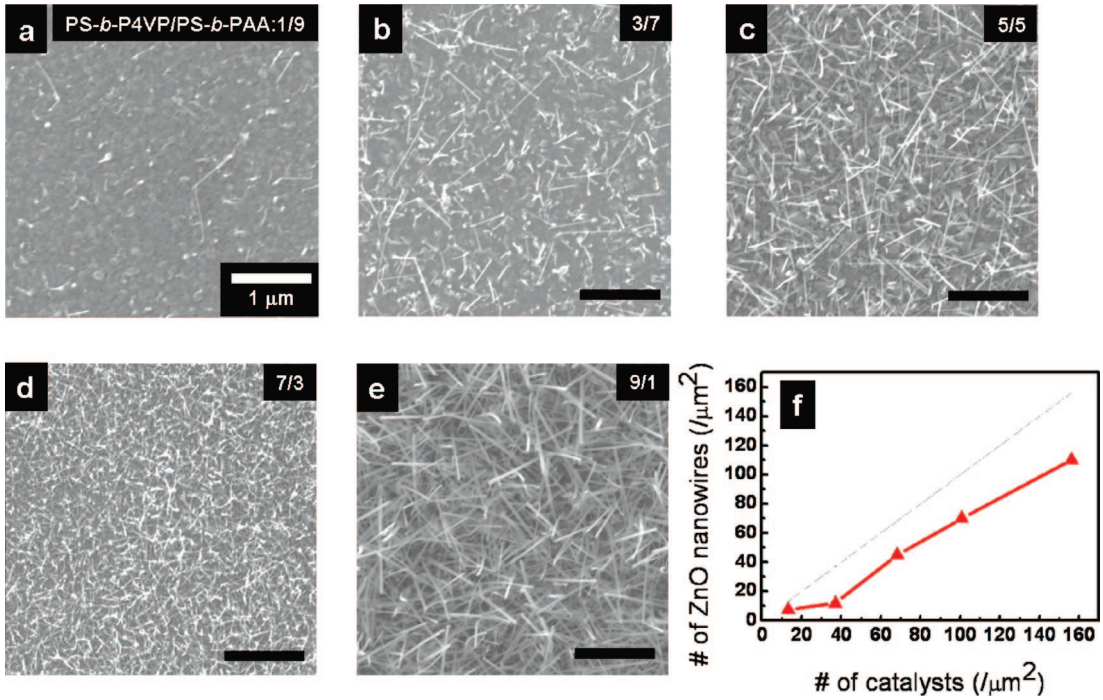

Figure 5. (a−e) SEM micrographs of the ZnO nanowires grown from the Au nanoparticles in the block copolymer micelles on Si substrates by VLS method. (f) A plot of area density of ZnO nanowires as a function of the area density of Au nanoparticles controlled by mixing PS-*b*-P4VP and PS-*b*-PAA micelles.

c in Figure 4 are frequently observed because of their delicate temperature dependence during solution preparation and nothing to do with the comicellization with PS-*b*-P4VP.

ZnO nanowires were successfully grown from the Au nanoparticle catalysts in the blend thin films by VLS method. Figure 5a−e showed SEM micrographs of ZnO nanowires on Si substrates whose area density was controlled by blending the two micelle solutions. The synthesis of ZnO catalyzed by Au nanoparticles was confirmed by a micrograph shown in Figure 6a where Au nanoparticles with approximately 30 nm in diameter was capped on the top of ZnO nanowires. The diameter and length of ZnO nanowires range from 20 to 30 nm, and from 3 to 5 μm, respectively. Both high-resolution TEM and selected area diffraction (SAD) pattern of ZnO nanowire in Figure 6b clearly exhibit a single-crystalline structure with its preferential growth along [001] direction. The fringe spacing in the TEM image is around 0.52 nm which corresponds to the (002) interplanar spacing. The crystalline structure of the nanowires also turns out to be typical hexagonal wurtzite ZnO (zinc blend) phase from X-ray diffraction as shown in Figure 6c.

With varying the blend ratio of PS-*b*-P4VP to PS-*b*-PAA micelle from 0.1 to 0.9, the surface coverage of ZnO nanowires increases. We estimated the area density of the nanowires on the basis of several frames of SEM micrographs for each blend ratio. Our method allows us to tune the area density of nanowires from approximately 15 to120 μm^{-2}. Compared with the area density of Au nanoparticles manipulated by blending the two block copolymer micelles, the density of nanoparticles is strongly correlated with that of the nanowires as shown in Figure 5f. As noticed, the correlation between the catalysts and the nanowires is not exactly linear but deviated below a linear proportion limit, indicative of the failure of the direct growth of one nanowire-

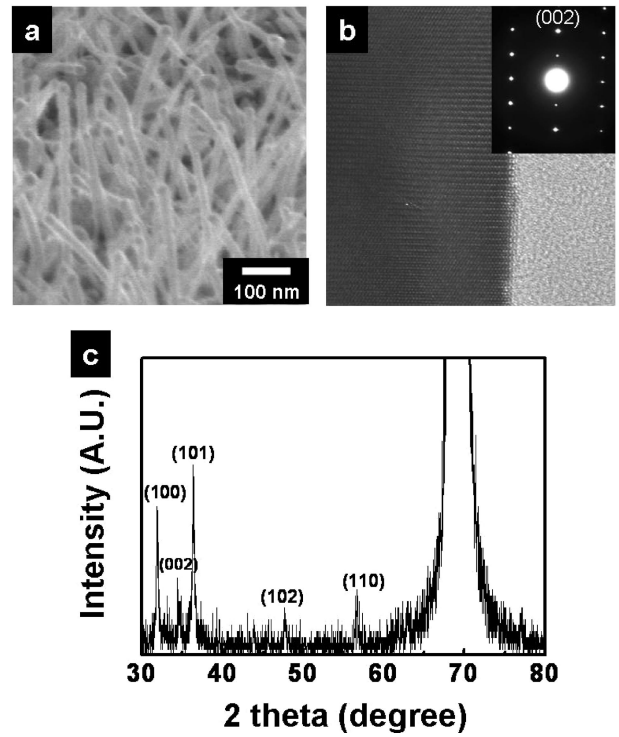

Figure 6. (a) SEM micrograph of the ZnO nanowires grown from the catalytic Au nanoparticles, which are clearly seen on the top of ZnO nanowires. (b) High-resolution TEM micrograph of a single-crystal ZnO nanowire. Inset of (b) displays a SAD pattern of (b). (c) XRD pattern of the ZnO nanowires.

to-one nanoparticle in the core of a micelle. In fact, at very low density of nanoparticles (e.g., the blend ratio 0.1), the area density of nanoparticles is almost the same as that of nanowires. When the blend ratio increases, the area density of nanowires becomes lower and lower than that expected.

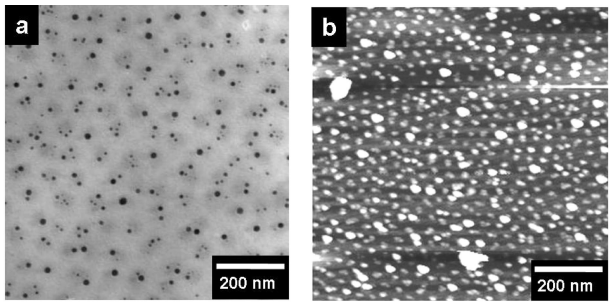

Figure 7. (a) Bright-field TEM and (b) AFM micrograph in height contrast of the PS-*b*-P4VP micelle film with $HAuCl_4$ loaded in P4VP blocks after heat treatment at 200 and 600 °C for 2 h, respectively. Coalescence of the raspberry type Au nanoparticles was apparent during heat treatment.

The deviation of the area density of nanowires from the linear correlation is mainly attributed to the interparticle merge between two Au nanoparticles in the micelles during nanowire synthesis. It is noted that the diameter of ZnO nanowires at low blend ratio(~20 nm) becomes larger to 30 nm when the blend ratio is greater than 0.5. Upon heating for ZnO synthesis, the raspberry type Au nanoparticles in the core of a micelle (Figure 3a) tend to merge with each other to form a single nanoparticle on which ZnO nanowire begins to grow. To confirm our speculation, we independently performed heating experiment with a monolayered PS-*b*-P4VP micelle film with $HAuCl_4$ loaded in P4VP blocks. A bright-field TEM micrograph in Figure 7a clearly indicates the formation of the Au nanoparticles coalesced from the much smaller raspberry type ones in the sample heat treated at 200 °C for 2 h with Au nanoparticles ranging from 15 to 20 nm in diameter. Further heat treatment at 600 °C for 2 h gave rise to Au nanoparticles more distributed in size with the maximum diameter of larger than 30 nm as shown in AFM image of Figure 7b. The larger 30 nm ZnO wires observed at high blend ratios were grown from the larger Au catalysts formed during heating by intermicelle diffusion. It is obvious that the intermicelle merge between two nanoparticles occurs more frequently when the average particle distance becomes short at the high blend ratios.

For further control of the area density of nanowires, we employed the micropatterning of the blended micelle films. In particular, the combination of our method with soft lithographic patterning techniques enables us to fabricate regularly spaced micropatterns of the blend micelle films where the area density of nanoparticles is again controlled. We directly spin coated a blend micelle solution on a prepatterned PDMS mold and subsequently transferred the formed monolayered blend film on a Si substrate as depicted in the schematic of Figure 8a. The rapid film formation by spin coating in our method is additionally beneficial because it offers the micropatterns with several tens of nanometer thick flat thin films by avoiding the inhomogeneous swelling of PDMS mold reported by others.[28,29] Figure 8 show the micropatterned monolayered micelles with the blend ratio of PS-*b*-P4VP to PS-*b*-PAA of 0.3. The larger PS-*b*-P4VP micelles are homogeneously mixed with the smaller PS-*b*-PAA micelles within the periodic line patterns of 450 nm in width. The selective loading of Au nanoparticles in P4VP cores is clearly apparent with the raspberry type nanoparticles aggregated in the core of approximately 50 nm in diameter, as shown in the inset of Figure 8c.

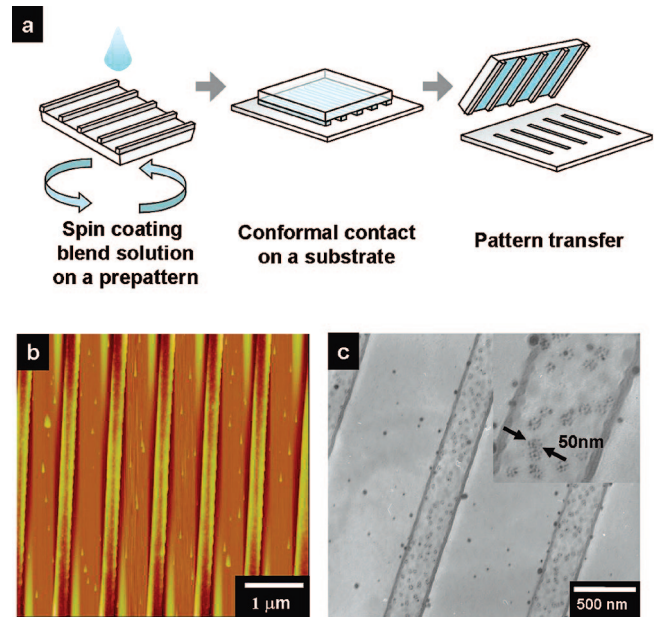

Figure 8. (a) Schematic of direct pattern transfer of a blended PS-*b*-P4VP/PS-*b*-PAA micelle film on a Si substrate. (b) AFM and (c) TEM micrographs of a PS-*b*-P4VP/PS-*b*-PAA (3/7) blend film micropatterned by the transfer method. The inset of (c) is a magnified bright-field TEM image visualizing the selective formation of Au nanoparticles in the P4VP cores in the micropatterns.

Conclusions

We tuned the area density of ZnO nanowires on a Si substrate by controlling the area density of the catalytic Au nanoparticles reduced from $HAuCl_4\ 3H_2O$ in the P4VP core of PS-*b*-P4VP copolymer micelles. Spin coating of blend solutions of PS-*b*-PAA and Au loaded PS-*b*-P4VP copolymer micelles with different blend ratios allowed us to avoid both the formation of hybridized micelles and the intermicelle diffusion of the metal nanoparticles and consequently to control the area density of the nanoparticles on which single crystal ZnO nanowires were grown with the diameter and length of 20−30 nm and 3−5 μm, respectively. The area density of ZnO nanowires ranging 15 to 120 μm^{-2} with a tuning capability of more than 800% was strongly correlated with that of Au nanoparticles in the micelles. Furthermore, we fabricated a micropattern of a monolayered blend micelle film with the controlled area density of Au nanoparticles by the direct transfer method.

Acknowledgment. This work was supported by Ministry of Commerce, Industry and Energy (MOCEI) through the project of NGNT (10024135-2005-11), the Korea Science and Engineering Foundation(KOSEF) grant funded by the Korea government (MEST) (R11-2007-050-03001-0 and R11-2005-008-00000-0) and Seoul Research and Business Development Program (10701). This work was supported by the Second Stage of Brain Korea 21 Project in 2006.

CM800719H

(28) Bennett, R. D.; Hart, A. J.; Miller, A. C.; Hammond, P. T.; Irvine, D. J.; Cohen, R. E. *Langmuir* **2006**, *22*, 8273.
(29) Yun, S. H.; Sohn, B. H.; Jung, J. C.; Zin, W. C.; Ree, M.; Park, J. W. *Nanotechnology* **2006**, *17*, 450.